Texila International Journal of Public Health
ISSN: 2520-3134
DOI: 10.21522/TIJPH.2013.12.03.Art008

Green Synthesis and Characterization of Cobalt Nanoparticles Using *Butea Monosperma* Flower Extract and their Biocompatibility Studies

Suraneni Venkata Dhruv Sudhakar Rao[1], S. Preetha[2], Sivasankari Sekar[3], Iadalin Ryntathiang[1], Archana Behera[1], Santosh Saravanan[1], Mukesh Kumar Dharmalingam Jothinathan[1*]

[1]*Centre for Global Health Research, Saveetha Medical College and Hospitals, Saveetha Institute of Medical and Technical Sciences (SIMATS), Saveetha University, Chennai, Tamil Nadu India*

[2]*Department of Forensic Medicine and Toxicology, Saveetha Medical College and Hospitals, Saveetha Institute of Medical and Technical Sciences (SIMATS), Saveetha University, Chennai, Tamil Nadu, India*

[3]*Department of Green Energy Technology, Microbial and Bioprospecting Bioenergy Laboratory, Madanjeet School of Green Energy Technologies, Pondicherry University, Kalapet, Puducherry – 605014*

Abstract

This study explores the green synthesis of cobalt nanoparticles (CoNPs) using Butea monosperma flower extract, highlighting their antibacterial efficacy, toxicity, and biocompatibility. Utilizing a plant-based reduction method, cobalt ions were reduced and stabilized by the bioactive compounds in the flower extract, forming CoNPs with notable uniformity and stability. Characterization techniques, including, UV-VIS spectroscopy, Fourier-transform infrared (FTIR) spectroscopy, and scanning electron microscopy (SEM) with energy-dispersive X-ray spectroscopy (EDAX), confirmed the formation and nature of the nanoparticles, which exhibited an average size of 10-20 nm. The synthesized CoNPs demonstrated significant antibacterial activity against both Gram-positive and Gram-negative bacteria, suggesting their potential as effective antimicrobial agents. Toxicity assessment using zebrafish, and brine shrimp lethality assay (BSLA), revealed that the nanoparticles exhibited minimal toxicity. Biocompatibility studies further indicated that CoNPs had no adverse effects on cellular morphology or proliferation, highlighting their suitability for biomedical applications. The eco-friendly synthesis method not only provides a sustainable approach to nanoparticle production but also enhances the potential for their safe application in medical and environmental fields. The findings underscore the promise of B. monosperma-mediated CoNPs as a viable alternative to chemically synthesized nanoparticles, with significant implications for antibacterial therapies and biocompatible materials.

Keywords: *Antibacterial Activity, Brine Shrimp Lethality Assay, Cobalt Nanoparticles, MTT Assay, Toxicology, Scratch Wound Healing Assay. Zebra Fish.*

Introduction

Nanotechnology has emerged as a groundbreaking field, offering precise control over materials at the atomic and molecular levels. Cobalt nanoparticles (CoNPs), with their unique magnetic properties and catalytic potential, have garnered significant interest for various applications [1]. Green synthesis methods, which employ environmentally friendly approaches like plant extracts or

Received: 11.06.2024 ***Accepted: 31.07.2024*** ***Published on: 30.09.2024***

****Corresponding Author: itsmemukesh@gmail.com***

microorganisms, synthesize CoNPs, enhancing their biocompatibility and reducing environmental impact [2, 3, 4].

CoNPs exhibit versatile applications across different sectors. In medicine, they show promise in targeted drug delivery, magnetic hyperthermia for cancer treatment, and as contrast agents in magnetic resonance imaging (MRI) [5, 6]. Often referred to as the flame tree, *Butea monosperma* belongs to the Fabaceae family and possesses a diverse spectrum of bioactive qualities, including antibacterial, antioxidant, and anti-inflammatory actions. In our study, we synthesized CoNPs using its extract, which is commonly known as the Palash tree in India [7].

In addition, nanoscale materials have been identified as innovative antibacterial agents. Various classifications of antimicrobial nanoparticles (NPs) and nanosized carriers for antibiotic delivery have demonstrated efficacy in laboratory settings for treating infectious diseases, including those caused by antibiotic-resistant strains [8]. According to [9] study shows that CoNPs synthesized using *Hibiscus cannabinus* leaf extract have significant antibacterial activity. The CoNPs have an average size of 20.88 nm and are effective against *Bacillus subtilis* and *Escherichia coli*.

Several Characterisation techniques have been applied to ascertain the characteristics of synthesized CoNPs. The composition is ascertained through the use of UV/Vis Spectroscopy, Fourier Transform Infrared Spectroscopy (FTIR), and Scanning Electron Microscopy (SEM) with Energy-Dispersive X-ray Spectroscopy (EDX) [10, 11].

Despite their promising applications, concerns regarding the cytotoxicity and biocompatibility of CoNPs persist [12]. Toxicology studies play a crucial role in assessing the safety profile of CoNPs and their impact on biological systems [13]. Previous research has highlighted the cytotoxic and genotoxic effects of CoNPs, emphasizing the need for comprehensive toxicity assessments to mitigate potential health risks [14].

Due to their genetic similarity to humans and transparent embryos that allow for real-time observation of developmental processes, researchers widely recognize zebrafish (*Danio rerio*) as valuable in vivo models for toxicity assessments [15]. The toxicity of CoNPs in zebrafish embryos is of particular interest, with studies focusing on parameters such as viability, hatch rate, and gross external phenotype [16]. Assessing the impact of CoNPs on zebrafish embryonic development provides crucial insights into their systemic effects and potential risks [17].

Zebrafish toxicology studies contribute significantly to understanding the safety profile of CoNPs and their suitability for biomedical applications [18]. Insights gained from these studies inform the development of strategies to mitigate potential toxicity risks associated with CoNP exposure [19]. Furthermore, studies on zebrafish toxicology pave the way for the development of safer nanomaterials with improved biocompatibility for therapeutic purposes [20].

In vitro studies are essential for evaluating the biocompatibility of CoNPs. Various cell lines are employed to assess parameters such as cell viability, reactive oxygen species (ROS) generation, and inflammation [21]. These studies provide valuable insights into the interactions between CoNPs and biological systems, informing their potential biomedical applications [22].

The toxicity assessment of CoNPs and their effect on biocompatibility studies represent critical areas of research in nanotoxicology [23]. By integrating in vitro and in vivo approaches, researchers aim to unravel the potential adverse effects of CoNPs and contribute to the development of safer nanomaterials for biomedical applications [24]. Zebrafish toxicology studies, in particular, provide valuable insights into the systemic effects of CoNPs and inform strategies to

enhance their biocompatibility and safety profile.

This study aims to evaluate the toxicity and biocompatibility of CoNPs using *B. monosperma* flower aqueous extract (BMFE) through various in vitro assays, including agar well diffusion technique, time-kill curve, protein leakage analysis, embryonic toxicology using zebrafish, toxicity assessment using brine shrimp lethality assay (BSLA), cell viability MTT assay, and scratch wound healing assay.

Materials and Methods

CoNPs are synthesized by using BMFE and characterized by various assays [7]. Figure 1 displays a graphical abstract of the green synthesis of CoNPs using plant extracts.

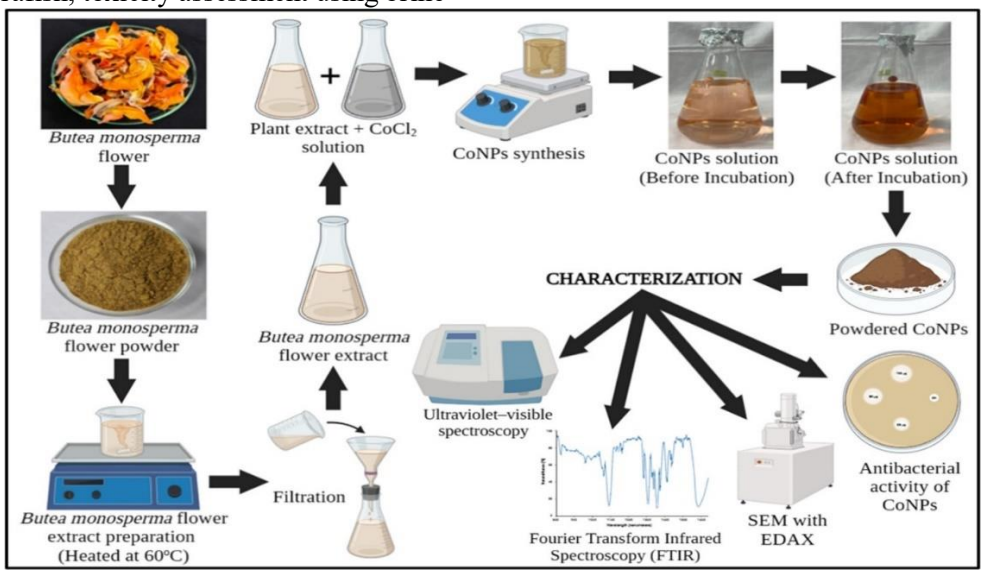

Figure 1. Graphical Abstract of Cobalt Nanoparticle Synthesis and its Characterization

Collection of Plant Sources

B. monosperma flowers (BMF) were collected from Chennai, Tamilnadu, India, in the month of June-July 2023. The samples were verified by the Centre for Advanced Studies in Botany at the University of Madras, Chennai, India.

Preparation of Extracts

The BMF was chopped into small pieces, washed 3 times with tap water, and subsequently air-dried in a shaded area for three days. Once the BMF were fully dried, they were ground into a fine powder and kept for future use. Subsequently, 25 g of BMF powder was poured into a 300 mL solution of double-distilled H_2O at 60°C for 20 mins. Afterwards, the extract was filtered using a muslin cloth and then further refined using a Whatman filter paper with a diameter of 125 mm. The filtered solution was subsequently stored at a temperature of 4°C. Further use.

Preparation of Cobalt Chloride Solution

A 5mM cobalt chloride ($CoCl_2$) solution was made by dissolving it in 300 mL of distilled water.

Synthesis of Cobalt Nanoparticles

To synthesize CoNPs, 10 mL of BMFE was combined with 90 mL of a $CoCl_2$ solution (5 mM) and agitated at 35°C. The acidity level of the reaction mixture was consistently checked and recorded. Subsequently, the reaction mixtures were incubated in a dark room on a rotating shaker at 40°C and a speed of 300 rpm for 3 hours. The visual evaluation of the reaction mixture's colour was followed by incubation at room temperature for 72 hours. After the incubation period, a total colour change was detected in the reaction mixture, suggesting the successful synthesis of nanoparticles. Conversely, the control containing solely $CoCl_2$ exhibited no alteration

in colour. Figure 2 depicts a graphical abstract of synthesised cobalt nanoparticle application.

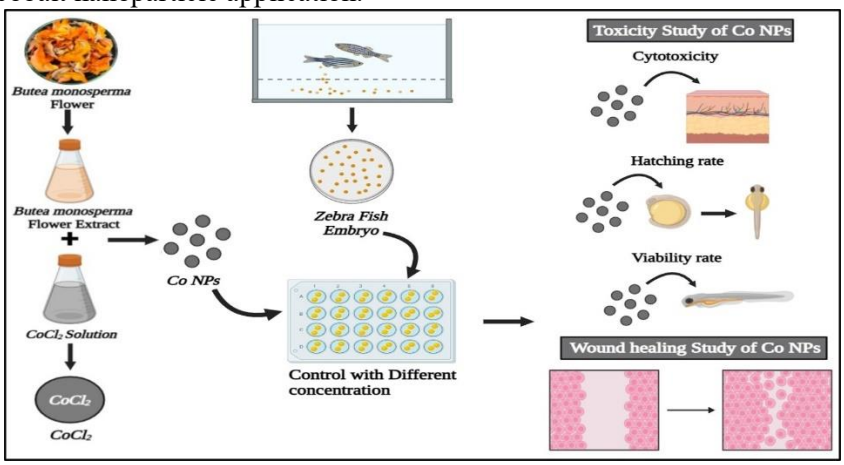

Figure 2: Graphical Abstract of Synthesised Cobalt Nanoparticle Application

Characterization of CoNPs

The CoNPs were characterized using UV- vis spectroscopy, FTIR spectroscopy, and SEM with EDAX. At first, synthesis was detected using UV-visible spectrophotometry in the range of 200-800 nm. The FTIR analysis, at 4000-400 cm^{-1}, successfully identified the specific functional groups present on the CoNPs. The morphology and purity were evaluated using SEM with EDAX.

Antibacterial Activity

Antibacterial activity was evaluated using CoNPs synthesized by BMFE using the agar well diffusion method. The bacterial culture selected one gram-positive (*Staphylococcus aureus*) and two negative bacteria (*E. coli and Pseudomonas sp.*) [25].

Time-Kill Curve Analysis

To assess the bactericidal properties of CoNPs, a time-kill curve was employed, following a methodology similar to the one described in the author's research work [26], their correlation with the growth patterns of the three above-mentioned bacteria was analyzed. This assay involved the cultivation of these pathogens in Mueller Hinton broth with varying concentrations of CoNPs (ranging from 100µg to 1000µg) while tracking their growth at specified time intervals.

To ensure consistent results, preliminary growth curves were established, ensuring that the pathogens reached from a stable early phase to a mid-log bacterial phase after a five-hour pre-incubation period in antibacterial-free Mueller Hinton Broth. A 0.5 McFarland inoculum of each pathogen was meticulously prepared in sterile phosphate-buffered saline (PBS) and derived from cultures grown on Mueller Hinton agar plates at 37°C for 18-20 hours. Subsequently, 30 µL of this inoculum was diluted in 15 mL of pre-warmed (37°C) antibacterial-free Mueller Hinton broth, and 90 µL of this resultant mixture was carefully dispensed into each well of a 96-well enzyme-linked immunosorbent assay (ELISA) plate. To each well, 10 µL of BMFE-CoNPs at five different concentrations were added, and an untreated control was also included in the assay for reference purposes.

Protein Leakage Analysis

The release of bacterial proteins into the supernatant was employed to assess the integrity of bacterial cells. Three bacterial suspensions (*E. coli, S. aureus, and Pseudomonas sp*), each with a volume of 10 mL, were treated with varying concentrations of BMFE- CoNPs (25, 50, and 100 µL). Bacterial suspensions served as positive controls, while ampicillin was used as standard.

The analysis of protein leakage was performed using an approach similar to the one described in the author's research [27].

Embryonic Toxicology Study on CoNPs Using Zebrafish

The zebrafish embryos were incubated in the culture medium as water and kept at a temperature of 26°C. Embryos that were chosen at random, 4 hours after fertilization (during the spherical stage), were kept in a 10 mL solution of zebrafish culture water. Viable embryos were placed on 96-well culture plates containing 0.2 mL of culture water. 0.1 mL of CoNPs synthesized by BMFE at various doses (5, 10, 20, 40, and 80 µg/mL) was applied to each well. The experiment consisted of three replicates, where the control group consisted of embryos in the culture media. The plates were placed in an incubator set at a temperature of 26°C. The progress of embryo and zebrafish larvae development was monitored at various time points after fertilization. The hatching and mortality rates were determined at 12-hour intervals based on the number of embryos that remained alive. The nanoparticles were seen to cause malformations in embryos under a microscope [28].

Toxicology Study Using Brine Shrimp

The brine shrimp lethality assay (BSLA) was used to evaluate the cytotoxicity of the CoNPs synthesized using the BMFE at different concentrations (5, 10, 20, 40, and 80 µg/mL). The assay was conducted using the approach described in prior work [29].

The Cell Viability MTT Assay

Fibroblast cells were cultured individually in 96-well plates at a density of 5×10^3 cells per well in DMEM media supplemented with 10% FBS and 1X antibiotic solution. The cells were then placed in a CO2 incubator at a temperature of 37°C with a CO2 concentration of 5%. The cells were rinsed with 100 µL of 1X PBS and then exposed to CoNPs. After that, they were incubated at 37°C with 5% CO2 for 24 h. Following the treatment, the liquid in the container was removed, and the cells were exposed to MTT (0.5 mg/mL in 1X PBS) at a temperature of 37°C for 4 h. After the incubation period, the media containing MTT was removed, the cells were rinsed with 100 µL of PBS, and the crystals that formed were dissolved in 100 µL of DMSO. The absorbance of the generated purple-blue formazan dye was quantified at a wavelength of 570 nm using a microplate reader. Cell vitality was determined based on the approach described in prior work [30].

To examine the impact of CoNPs produced by BMFE on cell morphology, a total of 200,000 normal fibroblast cells were evenly distributed in six-well plates and subjected to either CoNPs treatment or no treatment for 24 hours. After the treatment, the cells were rinsed with PBS and examined using an inverted phase contrast microscope.

Scratch Wound Healing Assay

3T3-L1 cells of 2×10^5 cells per well were placed onto six-well plate cultures. A wound was developed in the cell monolayer by scratching it with a 200 µl tip. The monolayer was then washed with PBS and images were taken using an inverted microscope. The cells were tested with CoNPs (100 µg/ml) for 24 hours, while the control cells were given a growth media without serum. The wound area photos were captured post-treatment, and the experiments were carried out three times for each treatment group [30].

Results

Ultraviolet-Visible Spectroscopy of Cobalt Nanoparticles

The "CoNPs BMFE" sample has an absorption spectrum in the 200–600 nm UV–Vis range shown in Figure 3. The absorbance peak is observable at approximately 220-230 nm, which suggests that the cobalt nanoparticles are undergoing electronic transitions. As the wavelength increases, the absorbance gradually

decreases, with the visible range having less absorbance and the UV region having more absorbance. The absorbance gets closer to zero as the wavelength gets closer to 600 nm, indicating little absorption in the visible range and pointing to general transparency. Charge transfer or electronic changes inside the nanoparticles are likely the cause of this notable UV absorption.

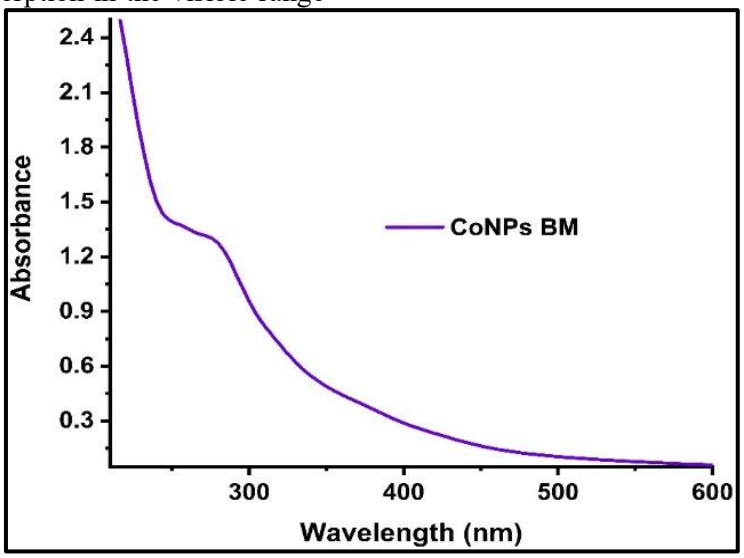

Figure 3. Ultraviolet-Visible Spectrum of Cobalt Nanoparticles Synthesized Using *B. Monosperma* Flower Aqueous Extract (BMFE)

FTIR Analysis of Cobalt Nanoparticles

CoNPs synthesized from *B. monosperma's* FTIR spectrum shown in Figure 4 illustrate the presence of several functional groups. The large peaks at 3825 and 3734 cm^{-1} indicate that water or hydroxyl groups may be the source of O-H stretching. The peak at 3261 cm^{-1} indicates that amines' N-H stretching is the cause. The C=C stretching indicated by the peak at 1601 cm^{-1} is most likely from aromatic compounds, while the peaks at 2085 and 1993 cm^{-1} suggest C≡C stretching from alkynes. The C-N stretching is represented by the 1251 cm^{-1} peak, and the C-O stretching is represented by the 1008 cm^{-1} peak. The nanoparticles' cobalt-oxygen interactions are characterized by metal-oxygen (M-O) bonds, which are confirmed by peaks in the 607 cm^{-1} range.

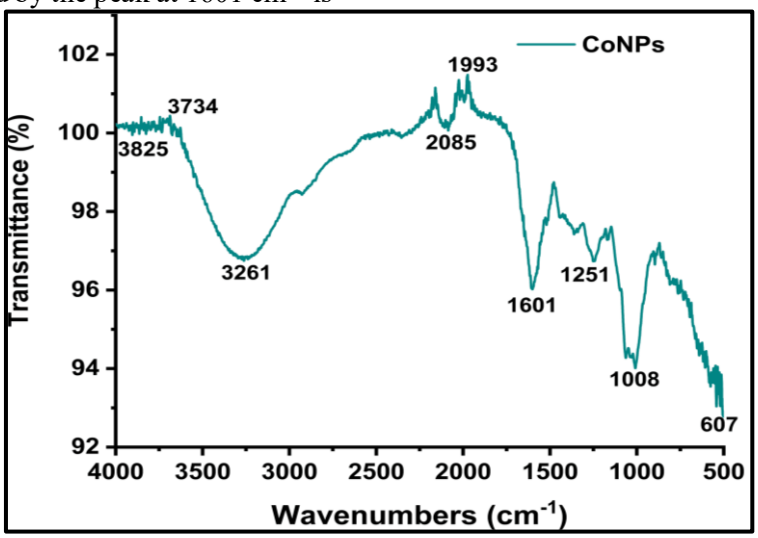

Figure 4. FTIR Spectrum of Cobalt Nanoparticles Synthesized Using B. *Monosperma* Flower Aqueous Extract (BMFE)

SEM with EDAX Analysis of Cobalt Nanoparticles

Figure 5A displays the SEM analysis results revealing that the synthesized BMFE-mediated CoNPs exhibit agglomerated spherical forms. These particles are scattered with an average size ranging from 10 to 20 nm. The elemental composition of the sample was revealed by the EDAX spectrum (Figure 5B), which displayed notable peaks for oxygen at 0.67 keV and cobalt at 6.93 keV, demonstrating oxygen's higher abundance. Based on the statistical analysis of the "Smart Quant Results" table, oxygen had a weight percentage of 76.26% and an atomic percentage of 92.21%. Its net intensity was 298.04 having a variance of 3.55%. For oxygen, the K-ratio, Z, A, and F values were, in that order, 0.7408, 1.0686, 0.9090, and 1.0000. Cobalt had a weight percentage of 23.74% and an atomic percentage of 7.79%. Its net intensity was 16.83 with an inaccuracy of 11.02%. Z, A, F, and K-ratio values were 0.1135, 0.7786, 0.6140, and 1.0000, in that order. This research provided information useful in material science by highlighting the majority of oxygen and a lower percentage of cobalt.

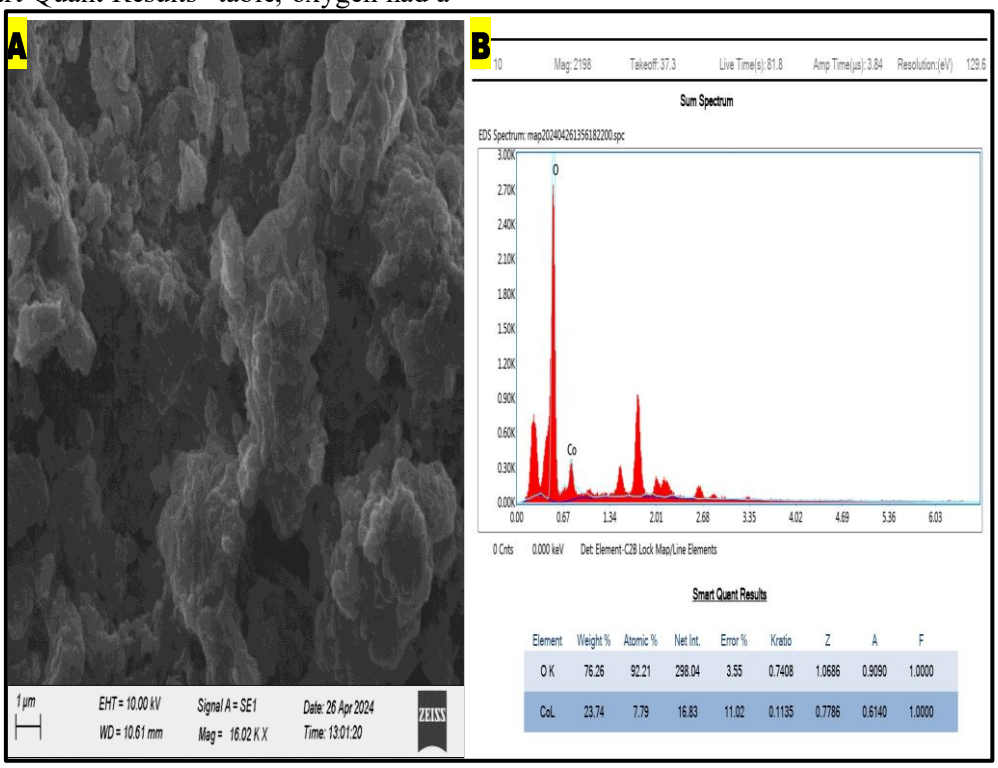

Figure 5. (A) Scanning Electron Microscopy Image, and (B) Dispersive X-ray Spectroscopy (EDAX) Spectrum of Cobalt Nanoparticles Synthesized Using *B. Monosperma* Flower Aqueous Extract (BMFE)

Antibacterial Activity of Cobalt Nanoparticles

Zones of inhibition (ZOI), which were the clear areas surrounding the antibacterial discs in Figure 6 showed how effective the antibacterial agent was at varying concentrations. The chemical was more successful in preventing bacterial growth in areas that were greater in size. Higher doses of $CoCl_2$ result in wider zones of inhibition, suggesting that it is efficient against the bacteria in this situation. The ZOI, or clear areas surrounding the antibacterial discs, demonstrate how well $CoCl_2$ works to block *S. aureus, E. coli, and Pseudomonas sp*. Greater suppression of bacterial growth was indicated by bigger zones, which were correlated with the concentration of $CoCl_2$. "100µg" was the most effective concentration, with the greatest inhibition zone; "50µg" and "25µg" were the next most effective. The antibiotics' efficiency was indicated by the zones of inhibition surrounding each disc,

which vary in size. The smallest zone was located around the 25-µg disc, the greatest zone was located around the 50-µg disc, and the largest zone was around the 100-µg disc. This pattern indicated that the bacterium was amenable to the NPs, with wider ZOI corresponding to higher concentrations.

The ZOI mm at 25, 50, and 100 µg/mL concentrations of *B. monosperma* (CoNPs) against *Pseudomonas, E. coli, and S. aureus*, together with a standard reference, illustrated the antibacterial activity of CoNPs. The concentration of CoNPs in µg/mL was represented by the x-axis, while the inhibition zones were displayed in mm on the y-axis. In all doses, *Pseudomonas sp* (blue), *E. coli* (red), and *S. aureus* (green) all showed comparable inhibitory zones that measured 8 to 10 mm. *Pseudomonas sp, E. coli, and S. aureus* stay around 8–10 mm, but the standard reference displayed a substantially greater ZOI for *E. coli*, at about 35 mm. At the quantities that were examined, the antibacterial activity of CoNPs was similar for all three species. However, especially when it comes to *E. coli*, the standard reference was significantly more powerful, as indicated in Figure 6D.

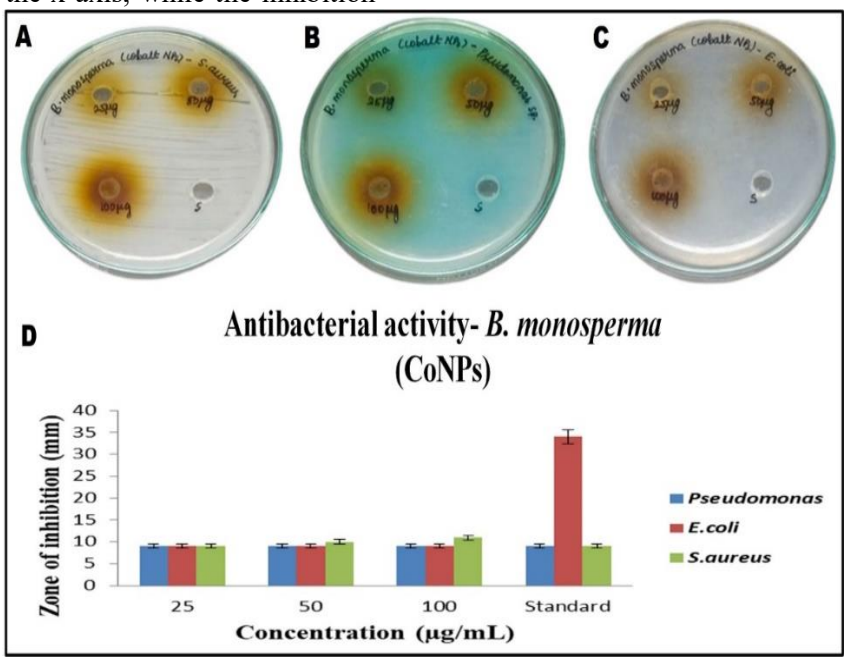

Figure 6. Antibacterial Activity (A) *S. Aureus*, (B) *Pseudomonas sp*., (C) *E. Coli*, and (D) Graphical Representation of Cobalt Nanoparticles Synthesized Using *B. Monosperma* Flower Aqueous Extract (BMFE)

Time-Kill Curve Analysis of Cobalt Nanoparticles

Over five hours, in Figure 7A, the graph showed how *B. monosperma* (CoNPs) reduced the number of *S. aureus*. Higher doses (100 µg/mL) are more effective than the usual antibacterial agent, although not as effective. Without treatment, the control exhibits increased bacterial growth, showing no antibacterial action.

Figure 7B demonstrates how *B. monosperma* (CoNPs) decreases *Pseudomonas sp* bacterial count during 5 hours; higher doses (100 µg/mL) are more efficient. In contrast to *B. monosperma*, the conventional antibacterial drug exhibits noticeably higher activity (CoNPs).

The graph in Figure 7C displays, about a standard and a control, the antibacterial action of *B. monosperma* CoNPs on E. coli over 5 hours at varying concentrations (25, 50, and 100 µg/mL). All treated groups, including the standard, show a drop in the number of bacteria, with greater doses of CoNPs producing a more notable reduction. The control group showed an increase in the number of bacteria.

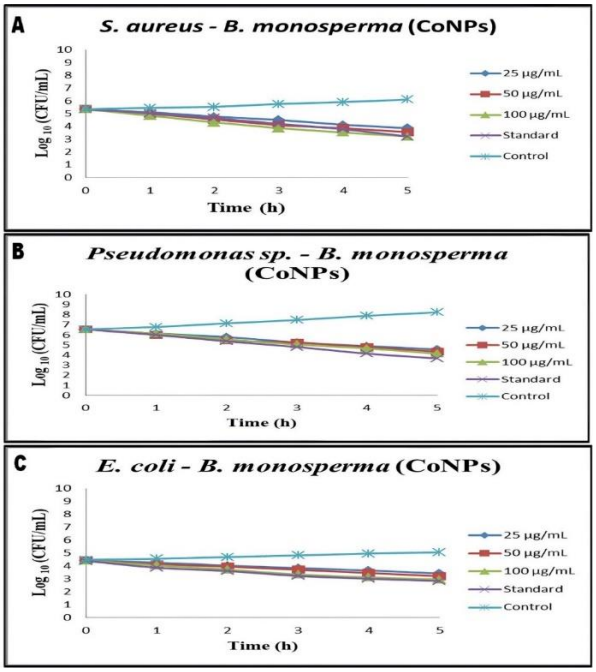

Figure 7. Time-Kill Curve Analysis of *B. Monosperma* (CoNPs) Against (A) *S. Aureus*, (B) *Pseudomonas sp*, and (C) *E. Coli*

Protein leakage analysis of cobalt nanoparticles

The protein leakage study of *B. monosperma* CoNPs at varying concentrations (25, 50, and 100 µg/mL) on three bacterial strains (*E. Coli, Pseudomonas sp.,* and *S. aureus*) is shown in Figure 8 about a standard and a control. All of the bacterial strains have optical density values that are comparable to the standard and rise with increasing CoNP concentrations; the control group exhibits the lowest optical density.

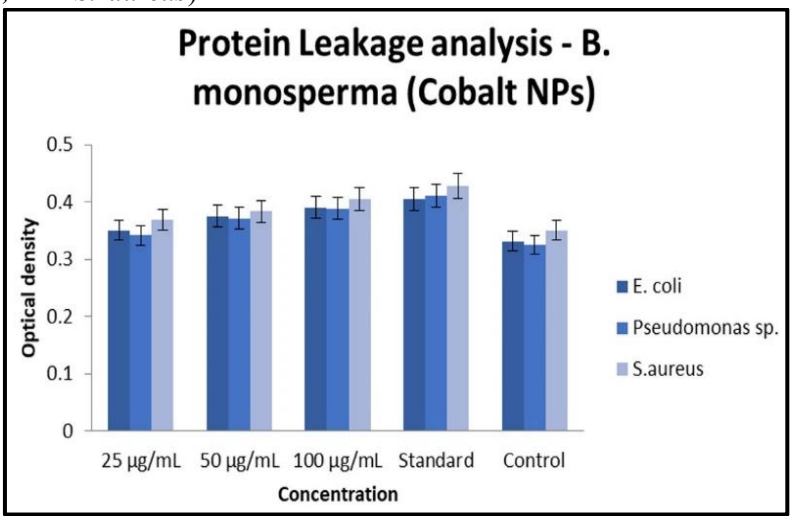

Figure 8. Protein Leakage Analysis of Cobalt Nanoparticles Synthesized Using B. *Monosperma* Flower Aqueous extract (BMFE)

Toxicity of Cobalt Nanoparticles in Zebrafish Embryos

Figure 9 depicts the various stages of zebrafish embryo development, including larval development. Regular cell division and general arrangement in the early embryonic stage, normal progression and segmentation in the late embryonic stage, and a well-formed head, eyes, somites, and tail in the larval stage all suggest

that CoNPs may not cause acute toxicity or significant developmental delays up to these stages. More investigation is necessary to determine any long-term consequences through molecular assays, specific developmental endpoints, hatching success rate, and survival rate.

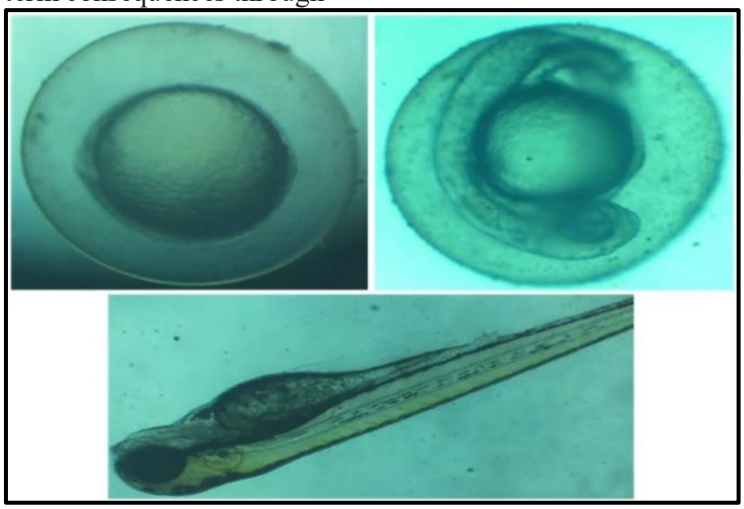

Figure 9. CoNPs Incorporated Phases of Zebrafish Embryo and Larval Developments

Hatching Rate of Zebrafish Egg Treated with CoNPs-BMFE

When compared to the control group, the hatching rates in Figure 10A show that CoNPs made from BMFE are not harmful at low concentrations (5-20 µg/mL). Hatching rates do, however, noticeably decline at higher dosages (40-80 µg/mL), suggesting considerable toxicity. This finding demonstrates that there is a concentration-based adverse effect on zebrafish embryo hatching.

Viability Rate of Embryo Treated with CoNPs-BMFE

Figure 10B shows that CoNPs made from BMFE don't affect the viability of zebrafish embryos at low doses (5-20 µg/mL), with viability rates that are the same as the control group. On the other hand, the nanoparticles exhibit increasing toxicity at higher doses of 40-80 µg/mL, as demonstrated by a drop in viability rates. This demonstrates a concentration-dependent harmful effect on zebrafish embryo viability.

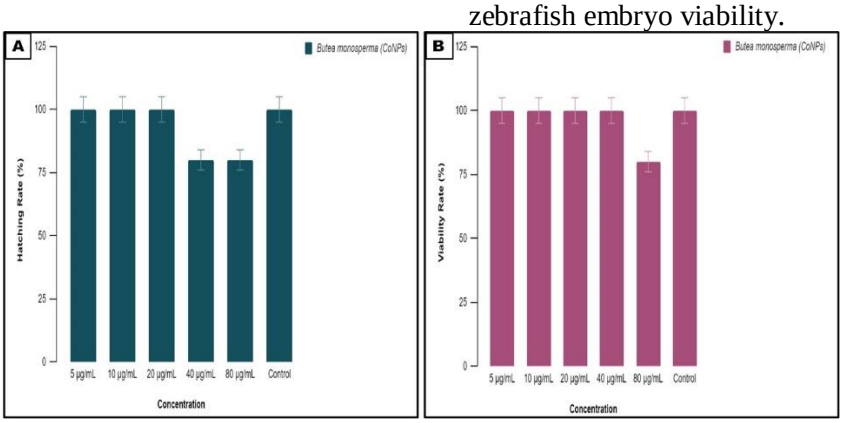

Figure 10. (A) Hatching Rate and (B) Viability Rate of Zebra Fish Egg Treated with CoNPs-BMFE

Hatching Rate of Eggs with BMFE

Figure 11A shows that the hatching rate of eggs with BMFE decreases as the concentration increases from 5 µg/mL to 80 µg/mL, with the control group showing the highest rate of hatching. Because there is a negative correlation between *B. monosperma*

concentration and hatching rate, this shows that higher concentrations inhibit hatching.

Viability Rate of Egg with BMFE

Figure 11B displays the percentage of cells that maintain viability following exposure to varying concentrations of BMFE. With a viability rate of about 100%, the control group has the highest rate of any treatment group. The other treatment groups' viability rates are considerably lower but still extremely close to 100%. This indicates that *B. monosperma* dosages ranging from 5 µg/mL to 80 µg/mL do not significantly lower cell viability when compared to the control group.

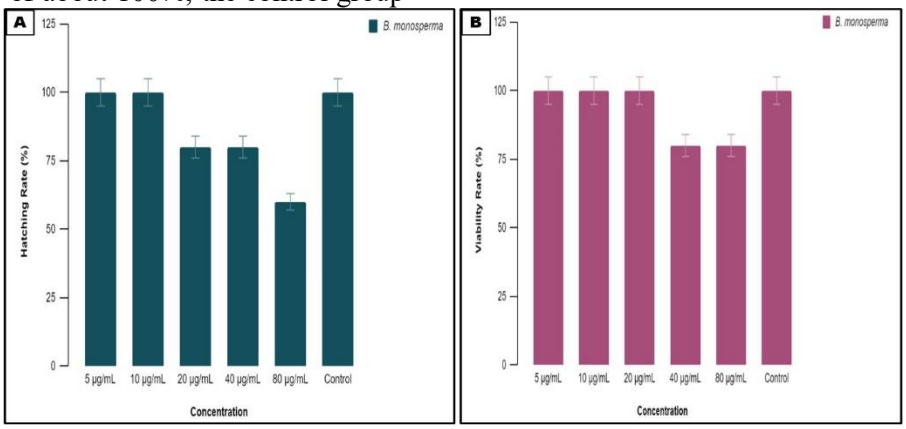

Figure 11. (A) Hatching Rate and (B) Viability Rate of Egg with BMFE

Cytotoxic Effect of CoNPs-BMFE

The cytotoxic effect of *B. monosperma* CoNPs during two days is shown in Figure 12A. It shows that the proportion stays almost 100% at lower concentrations (5, 10, and 20 µg/mL), but drastically drops to approximately 70% and 80% at higher concentrations that is 40 and 80 µg/mL. This indicates that the toxicity of CoNPs is dose-dependent, as evidenced by the fact that nauplii survival declines dramatically at higher concentrations while staying nearly 100% alive in the control group.

Cytotoxic Effect of BMFE

The bar graph is shown in Figure 12B, relative to a control, the cytotoxic effect of *B. monosperma* at various doses from 5, 10, 20, 40, and 80 µg/mL on live nauplii for two days. The percentage of live nauplii remains high at all concentrations and in the control, indicating that *B. monosperma* has negligible cytotoxicity at the measured concentrations.

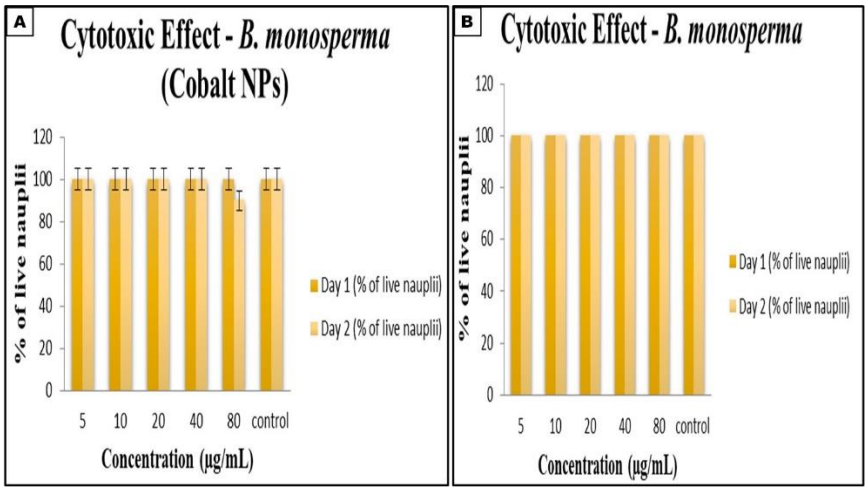

Figure 12. (A) Cytotoxic Effect of CoNPs-BMFE and (B) Cytotoxic Effect of BMFE

MTT Assay

The results of the MTT assay are shown in Figure 13 as a bar graph. It shows the percentage of living cells at different CONPs-BMFE concentrations (25, 50, 75, 100, 125, and 150 µg/mL) compared to a control. Up to 100 µg/mL, the data show that cell viability is high and similar to the control, but at 125 and 150 µg/mL, it considerably drops, indicating cytotoxic effects at higher dosages. CoNPs are not cytotoxic to normal fibroblast cells.

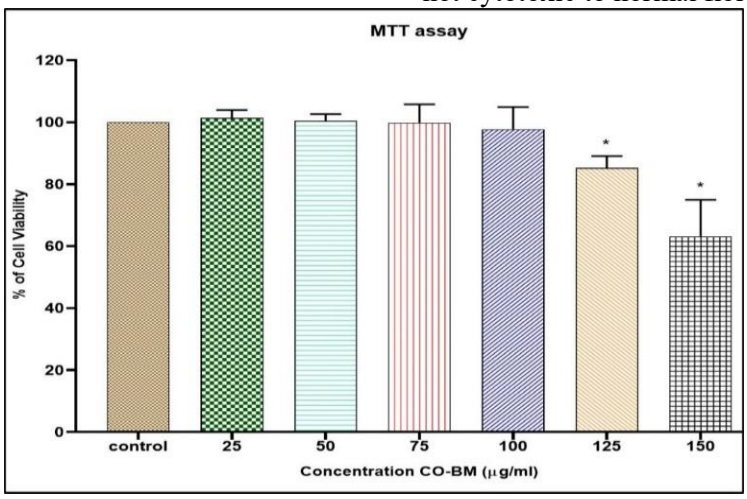

Figure 13. The Percentage of Cell Viability at Various CoNPs-BMFE Concentrations

Effect of CoNPs-BM on Cell Morphology of Osteosarcoma Cells (MG-63) of Human

The influence of CoNPs-BMFE on the morphology of human osteosarcoma cells (MG-63) was observed. After exposing cells to 100 µg/mL of CoNPs-BMFE for a day, they were looked at with the inverted phase contrast microscope shown in Figure 14. Following CoNPs-BMFE treatment, the number of cells shrank, and they exhibited cytoplasmic membrane blebbing. Figure 14A shows a control (MG-63) and Figure 14B tests samples of CoNPs-BMFE at 100 µg/mL.

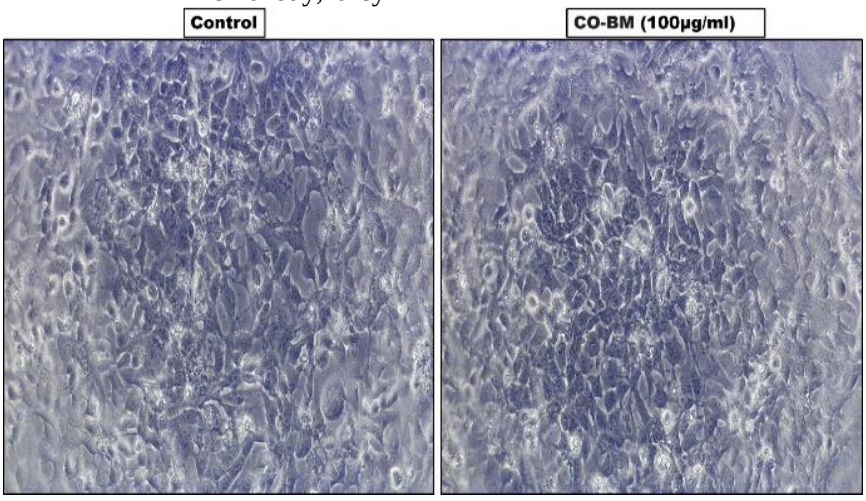

Figure 14. Effect of CoNPs-BM on Cell Morphology of Human Osteosarcoma Cells

Scratch Wound Healing Assay (3T3-L1)

Test for in vitro scratch wound healing. After injuring 3T3-L1 (mouse fibroblast) cells, a cell migration experiment was conducted 24 hours later both with and without therapy (CoNPs-BMFE 100 µg/ml). An inverted phase contrast microscope, as shown in Figure 15, was used to obtain images.

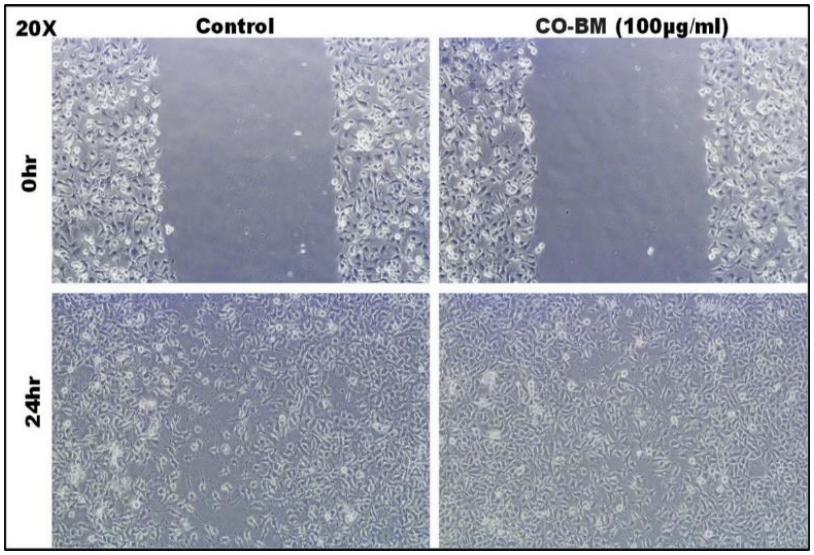

Figure 15. Scratch Wound Healing Assay- Migration of Cell

Discussion

This study synthesized CoNPs through a biosynthesis method using plant extract derived from *B. monosperma*. The UV-Vis analysis exhibited a distinct absorbance maximum at approximately 220-230 nm, which indicates electrical transitions in the nanoparticles. The absence of the peak towards longer wavelengths, which points toward transparency across the visible spectrum is due to the electrical nature of the NPs (CoNPs BMFE). According to the present work, and known investigations conducted on various metal nanoparticles synthesized by green synthesis approaches [7, 31].

FTIR analysis also revealed the presence of hydroxyl groups, amines, and aromatic compounds on CoNPs BMFE surface and others. These functional groups are believed to support both the stability and bioactivity of the NPs have been stated earlier in the synthesis of metal NPs mediated by plants [32, 33].

From the SEM with EDAX analysis, the levels of oxygen were recorded to be higher than cobalt and constituted the largest proportion of CoNPs BM's elemental components. The formulation of this composition follows recent papers on CoNPs synthesized from plant extracts [34] and also underscores the critical role of oxygen-rich conditions in NPs syntheses.

CoNPs BM exhibited antibacterial activity against different pathogens at different concentrations and the highest inhibition was observed against E. coli, S. aureus, and Pseudomonas. The increase in concentration resulted in more inhibition zones, and the antibacterial effectiveness at all the concentrations investigated in the present study agreed with the findings on metal nanoparticle-based antimicrobials from previous literature [35, 36].

As stated in most recent works, the investigation on the protein leakage prospects corroborated the antibacterial impact of CoNPs BMFE since it revealed a concentration-dependent enhanced protein leakage across bacterial cells, relating this to disturbances of the cell membranes caused by these NPs [37].

Considering all the factors, the realistic approach toward the synthesis of an embodiment of CoNPs for the treatment of clinically relevant diseases causing agents employing antimicrobial properties is the ecologically friendly synthesis of *B. monosperma* extract. The biological assessment and characterization of the study are in line with the most recent advancements in nanobiotechnology, suggesting the potential of

plant-mediated NPs for biomedical applications.

The current work examined the possible toxicity of BMFE-synthesized CoNPs on zebrafish embryos and different cell types. As with other studies [38, 39], the results suggest that CoNPs, at low concentrations (5-20 µg/mL), don't have a big effect on the survival and normal development of zebrafish embryos. We observe regular cell division and characteristic morphological traits throughout the embryonic and larval phases. However, the higher concentration ranges (40-80 g/mL) showed a negative impact, as evidenced by a lower hatching rate, viability, and deformities on the larvae, indicating a toxic activity based on concentration graduations.

These findings corroborate other studies that demonstrate the toxic impact of metal nanoparticles on aquatic species, contingent on the metal concentration. For instance, a study on the toxic effects of silver nanoparticles on zebrafish eggs demonstrated similar dose-dependent effects, with high concentrations exhibiting a strong toxic response and inhibiting development, while lower concentrations had negligible effects on egg development [1]. Regarding the above comparison and contrast, it is clear that nanoparticle concentration plays an important role in determining its toxicology.

The observed toxic effects of CoNPs are consistent with previous findings and are more evident at higher concentrations, as supported by the MTT assay data. Cell viability was good and similar to that of controls up to 100 µg/mL; however, at 125 and 150 µg/mL, cell viability was significantly reduced, and as such, there are some indications of cytotoxicity at higher concentrations. This is similar to what was found before about how metal oxide nanoparticles like zinc oxide and titanium dioxide are harmful; higher concentrations cause more oxidative stress, which damages cells [40, 41].

The scratch wound healing test with 3T3-L1 cells showed that CoNPs at 100 µg/mL slowed down cell migration, as the wound didn't close up as much after 24 hours. Similar studies of CoNPs that impaired cell motility through disruption of cytoskeleton dynamics agree with this migratory inhibition [42]. Furthermore, the degree to which MG-63 osteosarcoma cells' morphology changed after being exposed to CoNPs, including membrane blebbing, cell shrinkage, and a broken cytoskeleton, suggests that higher concentrations may be harmful to cells, which is in line with previous research [43].

However, the *B. monosperma* extract by itself did not show significant levels of cytotoxicity at the concentrations that were tested. It also had a small effect on the development of zebrafish embryos, as shown by the percentages of viable embryos and their growth. This implies that the CoNPs are mostly to blame for the observed toxicity in the combined CoNPs [31].

Conclusions

In conclusion, this research successfully highlights the green synthesis of CoNPs through the utilization of *B. monosperma* flower extract (BMFE). Characterization techniques such as UV-vis spectroscopy, SEM with EDAX, and FTIR confirmed the formation of distinct nanoparticles with a size range of 10–20 nm. This eco-friendly synthesis method minimizes the use of harmful chemicals, leveraging the inherent reducing and stabilizing factors in the flower extract. The synthesized CoNPs exhibited strong antibacterial effects against both Gram-positive and Gram-negative bacteria, indicating their potential applications in biomedicine and environmental science. However, the study on CoNP toxicity and biocompatibility revealed that higher concentrations of CoNPs led to minimal toxicity, as evidenced by reduced cell viability and higher levels of ROS. These findings highlight potential health risks associated with

CoNP exposure, necessitating careful consideration of dosage and safety measures in biomedical applications. The utilization of this green synthesis technique offers an ecologically friendly and economically effective method for producing CoNPs, combining sustainability with enhanced antibacterial properties. Additional research should investigate the mechanisms by which these biogenic nanoparticles exhibit antibacterial properties and explore their broader applications. Further studies are also needed to fully understand the impact of CoNPs on human health and to develop safer nanomaterials for medical use.

Acknowledgements

We would like to express our sincere gratitude to the Centre for Global Health Research, Saveetha Medical College and Hospitals, Saveetha Institute of Medical and Technical Sciences (SIMATS), Saveetha University, Chennai, India, for providing support for this research work. Finally, we thank all those who contributed to this work, directly or indirectly, and helped make this research possible.

Conflict of Interest

The authors declare that they have no conflict of interest.

Funding

The authors have no relevant financial or non-financial interests to disclose.

References

[1]. Vodyashkin, A. A., Kezimana, P., Prokonov, F. Y., Vasilenko, I. A., and Stanishevskiy, Y. M., 2022. Current Methods for Synthesis and Potential Applications of Cobalt Nanoparticles: A review. *Crystals*, *12*(2),272. https://doi.org/10.3390/cryst12020272

[2]. Alsaiari, N. S., Alzahrani, F. M., Amari, A., Osman, H., Harharah, H. N., Elboughdiri, N., and Tahoon, M. A., 2023. Plant and Microbial Approaches as Green Methods for the Synthesis of Nanomaterials: Synthesis, Applications, and Future Perspectives. *Molecules*, 28(1), 463. https://doi.org/10.3390/molecules28010463

[3]. Srivathsan, J., Sivakami, V., Ramachandran, B., Harikrishna, K.S., Vetriselvi, S. and Kumar, D.J.M., 2012. Synthesis of silver nanoparticles and its effect on soil bacteria. *J. Microbiol. Biotech. Res*, *2*(6), pp.871-874.

[4]. Khusnuriyalova, A. F., Caporali, M., Hey-Hawkins, E., Sinyashin, O. G., and Yakhvarov, D. G., 2021. Preparation of Cobalt Nanoparticles. *European Journal of Inorganic Chemistry*, 2021(30), 3023-3047. https://doi.org/10.1002/ejic.202100367

[5]. Pusta, A., Tertis, M., Crăciunescu, I., Turcu, R., Mirel, S., and Cristea, C., 2023. Recent Advances in the Development of Drug Delivery Applications of Magnetic Nanomaterials. *Pharmaceutics*, 15(7), 1872. https://doi.org/10.3390/pharmaceutics15071872

[6]. Farzin, A., Etesami, S. A., Quint, J., Memic, A., and Tamayol, A., 2020. Magnetic Nanoparticles in Cancer Therapy and Diagnosis. *Advanced Healthcare Materials*, 9(9), 1901058. https://doi.org/10.1002/adhm.201901058

[7]. Ryntathiang, I., Behera, A., Richard, T., and Jothinathan, M. K. D., 2024. An Assessment of the in Vitro Antioxidant Activity of Cobalt Nanoparticles Synthesized from Millettia Pinnata, Butea Monosperma, and Madhuca Indica Extracts: A Comparative Study. *Cureus*, 16(4), e59112. https://doi.org/10.7759/cureus.59112

[8]. Abass, A. A., Alaarage, W. K., Abdulrudha, N. H., and Haider, J., 2021. Evaluating the Antibacterial Effect of Cobalt Nanoparticles Against Multi-Drug Resistant Pathogens. *Journal of Medicine and Life*, 14(6), 823. https://doi.org/10.25122/jml-2021-0270

[9]. Kharade Suvarta, D., Nikam Gurunath, H., Mane Gavade Shubhangi, J., Patil Sachinkumar, R., and Gaikwad Kishor, V., 2020. Biogenic Synthesis

of Cobalt Nanoparticles using Hibiscus Cannabinus Leaf Extract and their Antibacterial Activity. *Research Journal of Chemistry and Environment*, 24(5), 9-13. https://www.researchgate.net/profile/Sachinkumar-Patil/publication/340844918

[10]. Cruz, J. C., Nascimento, M. A., Amaral, H. A., Lima, D. S., Teixeira, A. P. C., and Lopes, R. P., 2019. Synthesis and Characterization of Cobalt Nanoparticles for Application in the Removal of Textile Dye. *Journal of Environmental Management*, 242, 220-228. https://doi.org/10.1016/j.jenvman.2019.04.059

[11]. Fardood, S. T., Forootan, R., Moradnia, F., Afshari, Z., and Ramazani, A., 2020. Green Synthesis, Characterization, and Photocatalytic Activity of Cobalt Chromite Spinel Nanoparticles. *Materials Research Express*, 7(1), p.015086. https://doi.org/10.1088/2053-1591/ab6c8d

[12]. Kus-Liśkiewicz, M., Fickers, P., and Ben Tahar, I., 2021. Biocompatibility and Cytotoxicity of Gold Nanoparticles: Recent Advances in Methodologies and Regulations. *International Journal of Molecular Sciences*, 22(20), 10952. https://doi.org/10.3390/ijms222010952

[13]. Ansari, S. M., Bhor, R. D., Pai, K. R., Sen, D., Mazumder, S., Ghosh, K., Kolekar, Y. D., and Ramana, C.V., 2017. Cobalt Nanoparticles for Biomedical Applications: Facile Synthesis, Physiochemical Characterization, Cytotoxicity Behavior and Biocompatibility. *Applied Surface Science*, 414, 171-187. https://doi.org/10.1016/j.apsusc.2017.03.002

[14]. Bittner, M., Štern, A., Smutná, M., Hilscherová, K., and Žegura, B., 2021. Cytotoxic and Genotoxic Effects of Cyanobacterial and Algal Extracts—Microcystin and Retinoic Acid Content. *Toxins*, 13(2), 107. https://doi.org/10.3390/toxins13020107

[15]. Zhao, W., Chen, Y., Hu, N., Long, D., and Cao, Y., 2024. The Uses of Zebrafish (Danio rerio) as an in Vivo Model for Toxicological Studies: A Review Based on Bibliometrics. *Ecotoxicology and Environmental Safety*, 272, 116023. https://doi.org/10.1016/j.ecoenv.2024.116023

[16]. Modarresi Chahardehi, A., Arsad, H., and Lim, V., 2020. Zebrafish as a Successful Animal Model for Screening Toxicity of Medicinal Plants. *Plants*, 9(10),1345. https://doi.org/10.3390/plants9101345

[17]. Haque, E., and Ward, A. C., 2018. Zebrafish as a Model to Evaluate Nanoparticle Toxicity. *Nanomaterials*, 8(7), 561. https://doi.org/10.3390/nano8070561

[18]. Miyawaki, I., 2020. Application of Zebrafish to Safety Evaluation in Drug Discovery. *Journal of Toxicologic Pathology*, 33(4), 197-210. https://doi.org/10.1293/tox.2020-0021

[19]. Payne-Sturges, D. C., Scammell, M. K., Levy, J. I., Cory-Slechta, D. A., Symanski, E., Carr Shmool, J. L., Laumbach, R., Linder, S., and Clougherty, J. E., 2018. Methods for Evaluating the Combined Effects of Chemical and Nonchemical Exposures for Cumulative Environmental Health Risk Assessment. *International Journal of Environmental Research and Public Health*, 15(12), 2797. https://doi.org/10.3390/ijerph15122797

[20]. Cassar, S., Adatto, I., Freeman, J. L., Gamse, J. T., Iturria, I., Lawrence, C., Muriana, A., Peterson, R. T., Van Cruchten, S., and Zon, L. I., 2019. Use of Zebrafish in Drug Discovery Toxicology. *Chemical Research in Toxicology*, 33(1), 95-118. https://doi.org/10.1021/acs.chemrestox.9b00335

[21]. Frisch, E., Clavier, L., Belhamdi, A., Vrana, N. E., Lavalle, P., Frisch, B., Heurtault, B., and Gribova, V., 2023. Preclinical in Vitro Evaluation of Implantable Materials: Conventional Approaches, New Models and Future Directions. *Frontiers in Bioengineering and Biotechnology*, 11, 1193204. https://doi.org/10.3389/fbioe.2023.1193204

[22]. Othman, Z., Pastor, B. C., van Rijt, S., and Habibovic, P., 2018. Understanding Interactions Between Biomaterials and Biological Systems Using Proteomics. *Biomaterials*, 167, 191-204. https://doi.org/10.1016/j.biomaterials.2018.03.020

[23]. Egbuna, C., Parmar, V. K., Jeevanandam, J., Ezzat, S. M., Patrick-Iwuanyanwu, K. C., Adetunji, C. O., Khan, J., Onyeike, E. N., Uche, C. Z., Akram, M., and Ibrahim, M. S., 2021. Toxicity of Nanoparticles in Biomedical Application: Nanotoxicology. *Journal of Toxicology*, 2021(1), 9954443. https://doi.org/10.1155/2021/9954443

[24]. Witika, B. A., Makoni, P. A., Matafwali, S. K., Chabalenge, B., Mwila, C., Kalungia, A. C., Nkanga, C. I., Bapolisi, A. M. and Walker, R. B., 2020. Biocompatibility of Biomaterials for Nanoencapsulation: Current Approaches. *Nanomaterials*, 10(9),1649. https://doi.org/10.3390/nano10091649

[25]. Ryntathiang, I., Jothinathan, M. K. D., Behera, A., Saravanan, S., and Murugan, R., 2024. Comparative Bioactivity Analysis of Green-Synthesized Metal (Cobalt, Copper, and Selenium) Nanoparticles. *Cureus*, 16(3), e55933. https://doi.org/10.7759/cureus.55933

[26]. Munusamy, T., and Shanmugam, R., 2023. Green Synthesis of Copper Oxide Nanoparticles Synthesized by Terminalia chebula Dried Fruit Extract: Characterization and Antibacterial Action. *Cureus*, 15(12), e50142. https://doi.org/10.7759/cureus.50142

[27]. Anandan, J., and Shanmugam, R., 2024. Antioxidant, Anti-inflammatory, and Antimicrobial Activity of the Kalanchoe Pinnata and Piper Longum Formulation Against Oral Pathogens. *Cureus*, 16(4), e57824. https://doi.org/10.7759/cureus.57824

[28]. Rajeshkumar, S., Santhoshkumar, J., Vanaja, M., Sivaperumal, P., Ponnanikajamideen, M., Ali, D., and Arunachalam, K., 2022. Evaluation of Zebrafish Toxicology and Biomedical Potential of Aeromonas Hydrophila Mediated Copper Sulfide Nanoparticles. *Oxidative Medicine and Cellular Longevity*, 2022(1), 7969825. https://doi.org/10.1155/2022/7969825

[29]. Sankar, H. N., Shanmugam, R., and Anandan, J., 2024. Green Synthesis of Euphorbia Tirucalli-Mediated Titanium Dioxide Nanoparticles Against Wound Pathogens. *Cureus*, 16(2), e53939. https://doi.org/10.7759/cureus.53939

[30]. Ameena, M., Arumugham, M., Ramalingam, K., Rajeshkumar, S., and Perumal, E., 2023. Cytocompatibility and Wound Healing Activity of Chitosan Thiocolchicoside Lauric Acid Nanogel in Human Gingival Fibroblast Cells. *Cureus*, 15(8), e43727. https://doi.org/10.7759/cureus.43727

[31]. Ali, H., Dixit, S., and Alarifi, S., 2024. Biosynthesis and Screening of Cobalt Nanoparticles Using Citrus Species for Antimicrobial Activity. *Open Chemistry*, 22(1), 20240021. https://doi.org/10.1515/chem-2024-0021

[32]. Ali, S. G., Ansari, M. A., Alzohairy, M. A., Alomary, M. N., Jalal, M., AlYahya, S., Asiri, S. M. M. and Khan, H. M., 2020. Effect of Biosynthesized ZnO Nanoparticles on Multi-Drug Resistant Pseudomonas Aeruginosa. *Antibiotics*, 9(5), 260. https://doi.org/10.3390/antibiotics9050260

[33]. Kalanakoppal Venkatesh, Y., Mahadevaiah, R., Haraluru Shankaraiah, L., Ramappa, S., and Sannagoudar Basanagouda, A., 2018. Preparation of a CaO Nanocatalyst and its Application for Biodiesel Production Using Butea Monosperma Oil: An Optimization Study. *Journal of the American Oil Chemists' Society*, 95(5), 635-649. https://doi.org/10.1002/aocs.12079

[34]. Kumar, V., Harini, R., Anitha, G., and Nagaraju, G., 2024. Facile Green Synthesis of Zn Doped MoO3 Nanoparticles and its Photocatalytic and Photoluminescence Studies. *Journal of Molecular Structure*, 1312, 138494. https://doi.org/10.1016/j.molstruc.2024.138494

[35]. Mubraiz, N., Bano, A., Mahmood, T., and Khan, N., 2021. Microbial and Plant Assisted Synthesis of Cobalt Oxide Nanoparticles and their Antimicrobial Activities. *Agronomy*, 11(8), https://doi.org/1607.10.3390/agronomy11081607

[36]. Mmelesi, O. K., Masunga, N., Kuvarega, A., Nkambule, T.T., Mamba, B. B., and Kefeni, K. K., 2021. Cobalt Ferrite Nanoparticles and Nanocomposites: Photocatalytic, Antimicrobial Activity and Toxicity in Water Treatment. *Materials Science in Semiconductor Processing*, 123, 105523. https://doi.org/10.1016/j.mssp.2020.105523

[37]. Alyami, M. H., Fakhry, A. M., El Halfawy, N. M., Toto, S. M., Sedky, N. K., Yassin, H. A., Fahmy, S. A., and Mokhtar, F. A., 2023. Retama Monosperma Chemical Profile, Green Synthesis of Silver Nanoparticles, and Antimicrobial Potential: A Study Supported by Network Pharmacology and Molecular Docking. *RSC Advances*, 13(37), 26213-26228. https://doi.org/10.1039/D3RA05116A

[38]. Zafar, N., Madni, A., Khalid, A., Khan, T., Kousar, R., Naz, S. S. and Wahid, F., 2020. Pharmaceutical and Biomedical Applications of

Green Synthesized Metal and Metal Oxide Nanoparticles. *Current Pharmaceutical Design*, 26(45), 5844-5865. https://doi.org/10.2174/1381612826666201126144805

[39]. Siddiqi, K. S., Rahman, A., Tajuddin, N., and Husen, A., 2018. Properties of Zinc Oxide Nanoparticles and their Activity Against Microbes. *Nanoscale Research Letters*, 13, 1-13. https://doi.org/10.1186/s11671-018-2532-3

[40]. d'Amora, M., Schmidt, T. J. N., Konstantinidou, S., Raffa, V., De Angelis, F., and Tantussi, F., 2022. Effects of Metal Oxide Nanoparticles in Zebrafish. *Oxidative Medicine and Cellular Longevity*, 2022(1), 3313016. https://doi.org/10.1155/2022/3313016

[41]. Chen, J., Lei, L., Mo, W., Dong, H., Li, J., Bai, C., Huang, K., Truong, L., Tanguay, R. L., Dong, Q., and Huang, C., 2021. Developmental Titanium Dioxide Nanoparticle Exposure Induces Oxidative Stress and Neurobehavioral Changes in Zebrafish. *Aquatic Toxicology*, 240, 105990. https://doi.org/10.1016/j.aquatox.2021.105990

[42]. Yan, S., Qian, Y., Haghayegh, M., Xia, Y., Yang, S., Cao, R., and Zhu, M., 2024. Electrospun Organic/Inorganic Hybrid Nanofibers for Accelerating Wound Healing: A Review. *Journal of Materials Chemistry B*, 12, 3171-3190. https://doi.org/10.1039/D4TB00149D

[43]. Chakraborty, C., Sharma, A. R., Sharma, G., and Lee, S. S., 2016. Zebrafish: A Complete Animal Model to Enumerate the Nanoparticle Toxicity. *Journal of Nanobiotechnology*, 14,1-13. https://doi.org/10.1186/s12951-016-0217-6